Short Variable Sequence Acquired in Evolution Enables Selective Inhibition of Various Inward-Rectifier K^+ Channels

Yajamana Ramu, Angela M. Klem, and Zhe Lu*

Department of Physiology, University of Pennsylvania, 3700 Hamilton Walk, Philadelphia, Pennsylvania 19104

Received April 29, 2004; Revised Manuscript Received June 8, 2004

ABSTRACT: Tertiapin (TPN), a small protein toxin originally isolated from honey bee venom, inhibits only certain eukaryotic inward-rectifier K^+ (Kir) channels with high affinity. We found that a short (∼10 residues) sequence in Kir channels, located in the N-terminal part of the linker between the two transmembrane segments, is essential for high-affinity inhibition by TPN and that variability in the region underlies the great variation of TPN affinities among eukaryotic Kir channels. This short variable region is however not present in a bacterial Kir channel (KirBac1.1) or in many other types of prokaryotic and eukaryotic K^+ channels. Thus, the acquisition in evolution of the variable region in eukaryotic Kir channels has created the opportunity to selectively target the numerous types of Kir channel that play important physiological roles. We also show that TPN sensitivity can be readily conferred onto some Kir channels that currently have no known inhibitors by replacing their variable region with that from a TPN-sensitive channel. In heterologous expression systems, such acquired toxin sensitivity will allow currents carried by mutant channels to be readily isolated from interfering background currents. Finally we show that, in the heteromeric GIRK1/4 channels, the GIRK4 and not GIRK1 subunit confers the high affinity for TPN.

Inward-rectifier K^+ (Kir)[1] channels play many important physiological roles such as controlling the resting membrane potential, regulating cardiac and neuronal electrical activity, coupling insulin secretion to blood glucose levels, and maintaining electrolyte balance; mutations in certain Kir channels cause genetic diseases (*1*−*3*). Selective inhibitors of Kir channels are thus valuable therapeutic tools.

Despite the appealing reasons for attempting to develop specific inhibitors against medically significant Kir channels, the feasibility of such a strategy remains in doubt because of the perception that the targeted regions in K^+ channels are insufficiently diversified. To overcome that skepticism and encourage the development of effective medicines against specific Kir channels, we demonstrate that the sequence of the target region varies greatly among Kir channels and does exhibit inhibitor specificity. Previously, our group found that the honey bee toxin tertiapin (TPN) inhibits certain Kir channels (*4*). A subsequent alanine-scanning mutagenesis study showed that TPN inhibits the channels by binding to the linker region between the two transmembrane segments M1 and M2 (*5*). By studying chimeras between TPN-sensitive and -insensitive channels, we find here that variability of a ∼10-residue region in the M1−M2 linker underlies the variable TPN affinity among Kir channels, which could not have been learned from the alanine-scanning study itself. Sequence comparison shows that the small region varies significantly in both length and sequence among eukaryotic Kir channels and is not present in bacterial KirBac1.1. Thus, the apparent acquisition in evolution of the short variable region has created the condition required for the selective targeting of various Kir channels.

Investigation of Kir channel mechanisms is sometimes hampered by the lack of inhibitors for most subtypes of Kir channels, because currents through channels under examination often cannot be isolated from background currents, which confounds data analysis even in heterologous expression systems. The problem is especially acute in cases where channels of interest express poorly. The discovery of TPN and subsequent efforts to improve its characteristics proved beneficial only in studies of ROMK1 and certain GIRK channels (*6*, *7*). In the absence of inhibitors for other channel subtypes, a method for constructing mutant Kir channels with acquired TPN sensitivity and little or no alteration in functional characteristics would be highly desirable.

Last, the physiological roles of various GIRK channels in many tissues are being intensively studied. Whereas cardiac GIRK channels are formed by GIRK1 and GIRK4, different subunit combinations involving GIRK1 or GIRK4 may occur in other tissue types (*1*). Thus, the question of whether GIRK1 or GIRK4 actually underlies the apparent TPN sensitivity of the GIRK1/4 channels has been raised and needs clarification before TPN can be used to help identify GIRK channel subunit composition in certain cells (e.g., ref *8*). As shown below, our identification of a minimal sequence in Kir channels required for conferring TPN sensitivity represents an essential step toward fulfilling the three seemingly disparate goals delineated above: to develop

* To whom correspondence should be addressed: University of Pennsylvania, Department of Physiology, D302A Richard Building, 3700 Hamilton Walk, Philadelphia, PA 19104. E-mail: zhelu@mail.med.upenn.edu.

[1] Abbreviations: TPN, tertiapin; Kir, inward rectifier K^+ channel; Kv, voltage-gated K^+ channel; TPN_Q, tertiapin-Q; APMN, apamine; HEPES, 4-(2-hydroxyethyl)-1-piperazineethanesulfonic acid; ACh, acetylcholine; DTT, dithiothreitol; Tris, tris(hydroxymethyl)aminomethane; HPLC, high-performance liquid chromatography.

10.1021/bi049125x CCC: $27.50
Published on Web 07/31/2004

```
rKir 1.1(ROMK1) YVVAYVHKDLPEFY--PPDNRTPCVENINGMTSAFLFSLETQVTIGYGFRFVTEQCAT 155
mKir 2.1(IRK1)  WLIALLHGDLDT-----SKVSKACVSEVNSFTAAFLFSIETQTTIGYGFRCVTDECPI 156
rKir 3.1(GIRK1) WVIAYTRGDLNKAHV-G-N-YTPCVANVYNFPSAFLFFIETEATIGYGYRYITDKCPE 157
mKir 3.4(GIRK4) WLIAYVRGDLD--HV-GDQEWIPCVENLSGFVSAFLFSIETETTIGYGFRVITEKCPE 163
hKir 1.1        YAVAYIHKDLPEFH--PSANHTPCVENINGITSAFLFSLETQVTIGYGFRCVTEQCAT 155
hKir 2.1        WLIALLHGDLDA-----SKEGKACVSEVNSFTAAFLFSIETQTTIGYGFRCVTDECPI 156
hKir 3.1        WVIAYTRGDLNKAHV-G-N-YTPCVANVYNFPSAFLFFIETEATIGYGYRYITDKCPE 157
hKir 3.4        WLIAYIRGDLD--HV-GDQEWIPCVENLSGFVSAFLFSIETETTIGYGFRVITEKCPE 163
hKir 4.1        YLVAVAHGDLLEL-D-PPANHTPCVQVHTLTGAFLFSLESQTTIGYGFRYISEECPL 142
hKir 5.1        WLIAFHHGDLLN--D--PD-ITPCVDNVHSFTGAFLFSLETQTTIGYGYRCVTEECSV 145
hKir 6.2        WLIAFAHGDLAPS-EGTAE---PCVTSIHSFSSAFLFSIEVQVTIGFGGRMVTEECPL 144
hKir 7.1        YVLAEMNGDLELDHDAPPENHTICVKYITSFTAAFSFSLETQLTIGYGTMFPSGDCPS 133
KirBac 1.1      QLGDAPIAN----------------QSPPGFVGAFFFSVETLATVGYGDMHPQTVYAH 124
KcsA            AVLAERGAP----------------GAQLITYPRALWWSVETATTVGYGDLYPVTLWGR  89
MthK            FHFIEGE---------------------SWTVSLYWTFVTIATVGYGDYSPSTPLGM  73
KvAP            YIVEYPDPN----------------SSIKSVFDALWWAVVTATTVGYGDVVPATPIGK 223
Shaker          FAEAGSEN----------------SFFKSIPDAFWWAVVTMTTVGYGDMTPVGVWGK 456
Shab            FAEKDEKD----------------TKFVSIPEAFWWAGITMTTVGYGDICPTTALGK 637
Shal            YAEKNVNG----------------TNFTSIPAAFWYTIVTMTTLGYGDMVPETIAGK 384
Shaw            YAERIQPNP----------------HNDFNSIPLGLWWALVTMTTVGYGDMAPKTYIGM 391
```

FIGURE 1: Alignment of the sequence between M1 and M2 in mouse or rat Kir (mKir or rKir) channels used in the present studies. For comparison, also included are the sequences from human Kir (hKir) channels, a bacterial Kir channel (KirBac1.1), and other types of K^+ channels including bacterial KcsA, MthK, and KvAP, and *Drosophila* Kv channels Shaker, Shab, Shal, and Shaw.

subtype-specific therapeutic agents, to experimentally distinguish defined Kir channel currents from confounding background currents, and to dissect pharmacologically the tissue distribution of various Kir channel subtypes. Because the short region is in the turret (*9*), a mutation there often has little or no effect on conduction or gating properties of K^+ channels.

TPN, a 21-residue compact protein originally isolated from honey bee venom, inhibits cardiac GIRK1/4 (Kir3.1/3.4) and renal ROMK1 inward-rectifier K^+ (Kir1.1) channels with nanomolar affinity (*4*). In contrast, other Kir channels such as IRK1 (Kir2.1) are relatively TPN insensitive. Like scorpion toxins with voltage-gated K^+ (Kv) channels (*10*−*30*), TPN interacts 1:1 with Kir channels and inhibits them by binding to the external vestibule formed by the M1−M2 linker (*5*). The C-terminal portion of TPN (histidine 12−glycine 19) adopts an α-helical structure, whereas its N-terminal half acquires more extended conformations (*31*). Two pairs of disulfide bonds help hold the two parts together. Unlike scorpion toxins, which bind to Kv pores mainly via certain β sheets and not the α helix (*19*, *21*, *22*, *25*−*27*), TPN binds to a Kir pore with its α helix (*5*). Methionine residue 13, located at the N-terminal end of the α helix in TPN, readily undergoes oxidation under ambient conditions, significantly reducing its affinity for the channels (*6*). This technical inconvenience can be circumvented by replacing methionine 13 with glutamine to yield a TPN derivative called tertiapin-Q (TPN_Q). TPN_Q, though nonoxidizable under ambient conditions, binds to the channels with TPN-like affinity and selectivity. We therefore used TPN_Q to carry out the present study.

MATERIALS AND METHODS

Synthesis of cRNAs and Their Expression in Xenopus Oocytes. The cDNAs encoding mouse IRK1 (*32*), rat GIRK1 (*33*), mouse GIRK4 (*34*), and human muscarinic receptor 2 (*35*) were subcloned into the pGEM-HE vector (*36*), whereas rat ROMK1 cDNA (*37*) was cloned into a pSPORT plasmid (Gibco-BRL). All mutant cDNAs were obtained through PCR-based mutagenesis and confirmed by DNA sequencing. All cRNAs were synthesized using T7 polymerase (Promega)

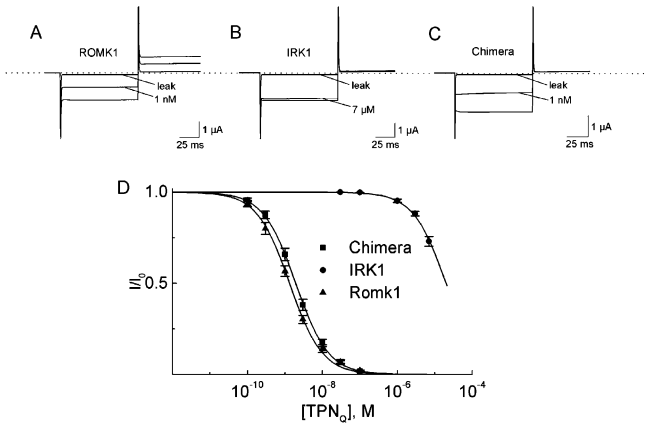

FIGURE 2: Inhibition of ROMK1, IRK1, and a chimeric channel by TPN_Q. (A−C) Currents of ROMK1, IRK1, and a chimera in which the M1−M2 linker of IRK1 is replaced by that of ROMK1, recorded in the absence or presence of TPN_Q at the concentrations indicated. Background leak currents are obtained as described in the Materials and Methods. Dashed lines indicate zero current levels. (D) Fraction of current not blocked (mean ± SEM; $n = 5-7$) plotted against the TPN_Q concentration. The curves through the data are fits of the equation $I/I_O = K_d/(K_d + [TPN_Q])$, yielding K_d values of 1.3 ± 0.1 nM, 20.0 ± 0.1 μM, and 1.9 ± 0.1 nM for ROMK1, IRK1, and the chimeric channel, respectively.

from the cDNAs linearized with *Nhe*I, except in the case of ROMK1, where *Not*I was used to linearize the plasmid.

Oocytes harvested from *Xenopus laevis* were digested with collagenase (2 mg/mL) in a solution containing 82.5 mM NaCl, 2.5 mM KCl, 1 mM $MgCl_2$, and 5 mM HEPES (pH 7.6) and agitated on a platform shaker at 80 rpm for 90 min. The oocytes were then rinsed thoroughly with and stored in a solution containing 50 μg/mL gentamicin, 96 mM NaCl, 2 mM KCl, 1.8 mM $CaCl_2$, 1 mM $MgCl_2$, and 5 mM HEPES (pH 7.6). Defolliculated oocytes were selected at least 2 h after the collagenase digestion. To express the channels, the coding RNA was injected into oocytes, except in the case of the GIRK1/4 channel, where cRNAs encoding GIRK1, GIRK4, and the muscarinic receptor were co-injected. All injections were carried out at least 16 h after the collagenase treatment. The injected oocytes were stored at 18 °C.

Channel Recording. All channels were studied using a two-electrode voltage clamp amplifier (Oocyte Clamp OC-725C,

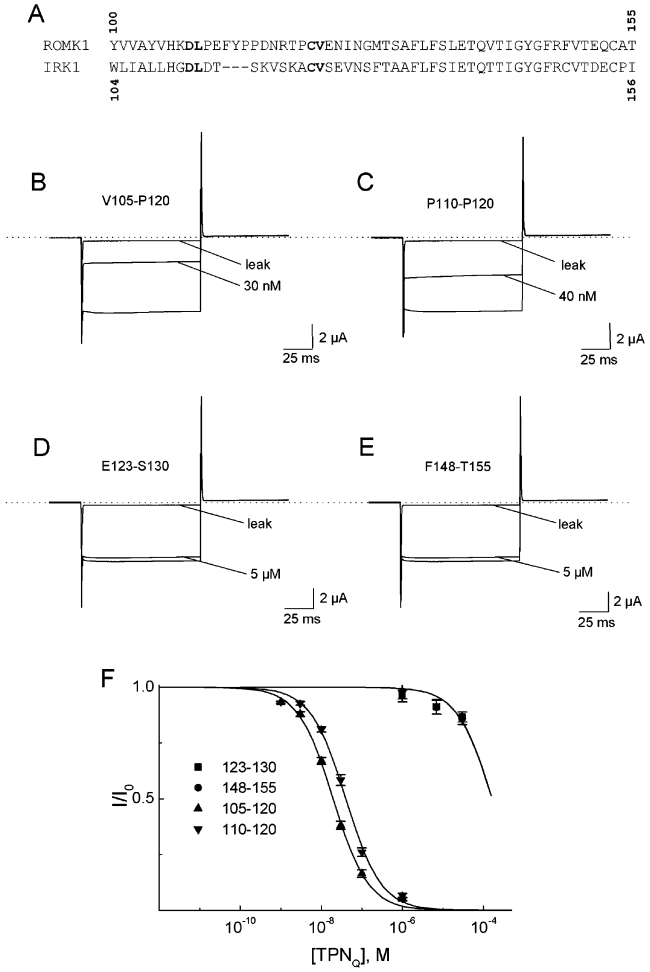

FIGURE 3: Inhibition of four chimeric channels by TPN_Q. (A) Alignment of the M1−M2 linker sequence between ROMK1 and IRK1. (B−E) Currents of four chimeric channels in which part of the M1−M2 linker in IRK1 is replaced by the indicated counterpart from ROMK1, recorded in the absence or presence of TPN_Q at the concentrations indicated. (F) Fraction of current not blocked (mean ± SEM; $n = 4-5$) plotted against the TPN_Q concentration. The curves through the data for the mutant IRK1 channels with ROMK1 sequences V105−P120 or P110−P120 are fits of the equation described in Figure 2, yielding K_d values of 19.3 ± 0.1 or 38.4 ± 0.3 nM. The curves through the remaining two data sets are hand-drawn.

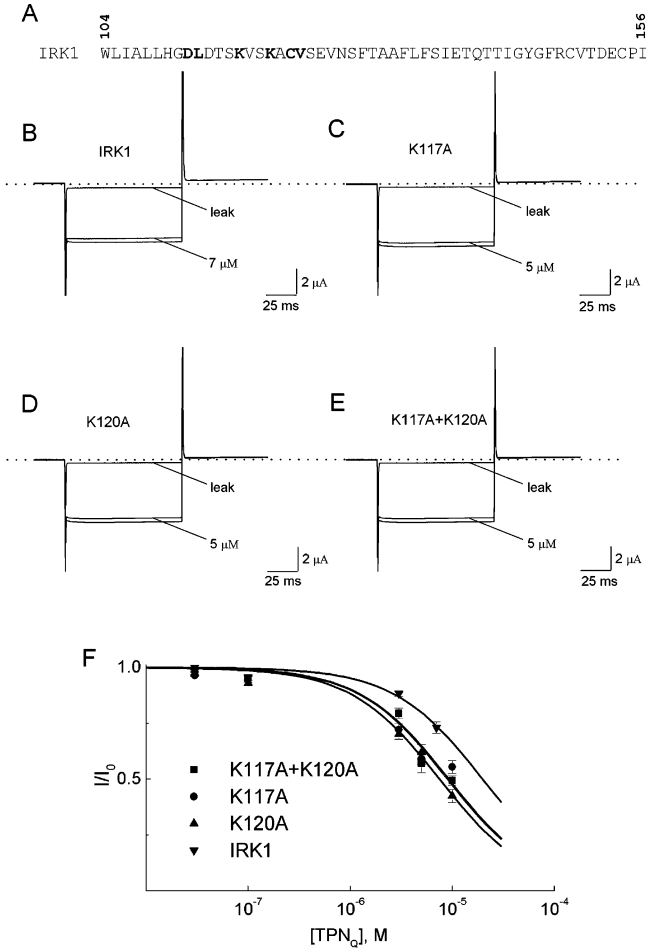

FIGURE 4: Effects of alanine mutation at lysine residues in the M1−M2 linker of the IRK1 channel. (A) Sequence of the M1−M2 linker in IRK1. (B−E) Currents of wild-type IRK1 channels or its mutants in which one or both lysine residues within the M1−M2 linker (bolded in A) are replaced by alanine, recorded in the absence or presence of TPN_Q at the concentrations indicated. (F) Fraction of current not blocked (mean ± SEM; $n = 5-6$) plotted against the TPN_Q concentration. The curves through the data are fits of the equation described in Figure 2, yielding K_d values of 20.0 ± 0.1, 6.6 ± 0.6, 6.9 ± 0.5, and 7.3 ± 0.7 μM for wild-type and mutant channels containing K117A, K120A, and K117A + K120A, respectively.

Warner Instruments Corp.). The resistance of electrodes filled with 3 M KCl was ~0.3 MΩ. To elicit channel current, the oocyte membrane potential was stepped to −80 mV and then to +80 mV from a holding potential of 0 mV. Background leak currents were obtained by exposing oocytes to solutions containing TPN_Q at concentrations $>100K_d$. For channels with very low affinity for TPN_Q, such as IRK1, the background leak currents were estimated in a bath solution containing 100 mM Na^+ (Cl^- + OH^-), 0.3 mM $CaCl_2$, 1 mM $MgCl_2$, and 10 mM HEPES (pH 7.6 adjusted with NaOH). In either case, the background current, whose amplitude is comparable to that in oocytes not injected with cRNA, does not inwardly rectify.

The bath solution contained 100 mM K^+ (Cl^- + OH^-), 0.3 mM $CaCl_2$, 1 mM $MgCl_2$, and 10 mM HEPES (pH 7.6 adjusted with KOH). To activate the GIRK1/4 channels coexpressed with M2 receptors, 150 μM ACh was included in the bath solution. The concentration of TPN_Q was calculated from the absorbance at 280 nm using an extinction coefficient of 6.1 mM^{-1} cm^{-1} (*4*), whereas that of apamine (APMN) or of the construct formed by joining the N-terminal half of TPN_Q to the C-terminal half APMN (see the Results) was estimated using 0.4 mM^{-1} cm^{-1}.

Synthesis, Mass Determination, and Purification of Toxins. All toxin peptides were synthesized with a multipeptide synthesizer, and the mass of synthesized products was confirmed with MALDI spectrometry (Keck Biopolymer Facility, Yale University). All synthetic peptides have a C-terminal amide group. For proper folding, each synthetic peptide was dissolved in a solution containing 1 mM DTT and 10 mM Tris (pH 8.0) (*4*). After DTT became oxidized, the peptide spontaneously adopted the active conformation and was purified on a reverse-phase HPLC column (C18) using a linear-methanol gradient (1% per minute).

RESULTS

Identification of a Short Sequence Underlying TPN_Q Selectivity in Kir Channels. TPN_Q inhibits certain Kir

channels by binding to the M1−M2 linker region whose alignment among various homologous Kir channels is shown in Figure 1. For technical simplicity, we first examined how TPN_Q interacts with two inward rectifiers, ROMK1 and IRK1, which exhibit very different affinities. Parts A and B of Figure 2 show that TPN_Q at 1 nM inhibits about half of the ROMK1 current, whereas it barely inhibits the IRK1 current even at 7 μM. To start identifying the sequence that determines channel selectivity for TPN_Q, we replaced the entire region between M1 and M2 in IRK1 with its counterpart from ROMK1 (Figure 1). The chimeric channel is approximately as sensitive to TPN_Q as ROMK1 itself (parts A and C of Figure 2). Figure 2D plots the normalized currents carried by ROMK1, IRK1, and the chimeric channel against the concentration of TPN_Q. The curves through the data are fits of the equation for a 1:1 binding model, yielding K_d values of 1.3 nM, 20 μM, and 1.9 nM for ROMK1, IRK1, and the chimeric channel, respectively. Thus, affinities of ROMK1 and the chimeric channel for TPN_Q are comparable and much higher than that of IRK1.

Pore-blocking toxins bind to K^+ pores by interacting with residues in regions N terminal to the pore helix or C terminal to the signature sequence trailing the pore helix. Residues in the former region shape the turrets lining much of the extracellular vestibule of the ion conduction pore, whereas those in the latter region surround the external opening of the pore (*9*). We further divided the N-terminal region into two parts, corresponding to V105−P120 and E123−S130, respectively, in ROMK1 (Figure 3A). The two residues (CV) that connect the parts are conserved between ROMK1 and IRK1. Substituting V105−P120 from ROMK1 for the corresponding sequence in IRK1 increases the affinity of the latter for TPN_Q by 1000-fold (K_d decreases from 20 μM to 19 nM; compare parts B and D of Figure 2 with parts B and F of Figure 3). In contrast, substituting E123−S130 or the distal region F148−T155 alone has little effect on the affinity of IRK1 for TPN_Q (parts B and D of Figure 2 versus parts D−F of Figure 3). Interestingly, a shorter region corresponding to P110−P120 of ROMK1, flanked by two pairs of conserved residues (DLX...XCV; Figure 1), appears to be a cassette with sequences that vary among eukaryotic Kir channels. This region is however absent in the prokaryotic KirBac1.1. Substituting only this variable region from ROMK1 (P110−P120) for its counterpart in IRK1 lowers the K_d of IRK1 for TPN_Q from 20 μM to 38 nM (parts C and F of Figure 3), an affinity comparable to that (K_d = 19 nM) of the mutant containing the longer ROMK1 sequence V105−P120 (parts B and F of Figure 3).

There are two lysine residues in the variable region of IRK1 (Figure 4A), which raises the question whether the extremely low affinity of IRK1 for TPN_Q merely reflects energetically unfavorable interactions between these positively charged residues and those in TPN_Q (one histidine, one arginine, and four lysine residues). To examine this, we replaced one or the other or both lysine residues in IRK1 with alanine; all three mutants are almost as insensitive to TPN_Q as wild-type IRK1 is (parts B−F of Figure 4).

The variable region in IRK1 might conceivably adopt a special conformation and incidentally hinder the binding of TPN_Q. To test this possibility, we made an IRK1 construct lacking the variable region (DTSKVSKA; Figure 1). This deletion mutant, like the wild-type IRK1 channel, conducts

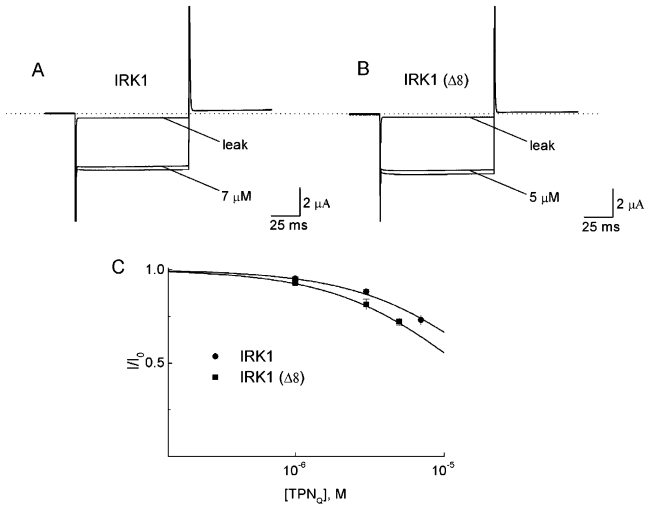

FIGURE 5: Effect of deleting the variable region in IRK1 on TPN_Q inhibition. (A and B) Currents of wild-type and mutant (Δ8) IRK1 channels in which the variable region (DTSKVSKA; Figure 1) is deleted, recorded in the absence or presence of TPN_Q at the concentrations indicated. (C) Fraction of current not blocked (mean ± SEM; n = 4−5) plotted against the TPN_Q concentration. The curves through the data are fits of the equation described in Figure 2, yielding K_d values of 20.0 ± 0.1 and 10.0 ± 0.1 μM for the wild-type and mutant channels, respectively.

K^+ current in an inwardly rectifying manner and is relatively insensitive to TPN_Q (K_d = 10 μM; Figure 5).

To examine further the interaction between TPN_Q and the variable region, we performed thermodynamic mutant cycle analysis, comparing how TPN_Q and a mutant thereof block the wild-type and a mutant IRK1. The construct TPN_Q-APMN is a mutant TPN_Q molecule where, for reasons discussed below, the C-terminal half is replaced by that from apamine (APMN) (Figure 6A). The mutant IRK1 contained variable region P110−P120 from ROMK1 and, therefore, exhibited high affinity for TPN_Q.

TPN and APMN are toxin isoforms from honey bee venom (Figure 6A). Their C-terminal halves adopt an α-helical conformation, whereas their N-terminal halves are more extended (*31*, *38*). Two disulfide bonds help hold the two structural elements together. Previous studies have shown that only TPN and not APMN inhibits certain Kir channels with high affinity and that the α helix in TPN is the channel-binding domain (*4*, *6*). To test whether the variable region in the Kir channels interacts with TPN_Q, we replaced the C-terminal α helix of TPN_Q by that from APMN. Because it is the α helix that actually binds to the channel, the TPN_Q-APMN chimera is expected to act like APMN and not TPN_Q. Indeed, APMN and the chimera block IRK1 with nearly identical (and low) affinity ($K_d \approx$ 20 μM), regardless of whether that variable region of the channel is replaced by P110−P120 of ROMK1 (parts B−F of Figure 6). Consequently, the value of the energetic coupling coefficient Ω (*25*) computed with K_d values of wild-type and mutant IRK1 channels for APMN and the TPN_Q-APMN chimera is near unity (top part of Figure 7). In contrast, the Ω value is ∼450 when computed with K_d values of wild-type and mutant IRK1 channels for TPN_Q and the TPN_Q-APMN chimera (bottom part of Figure 7). These results support a model where the α helix in TPN_Q interacts with the variable region in the channel to produce high-affinity inhibition.

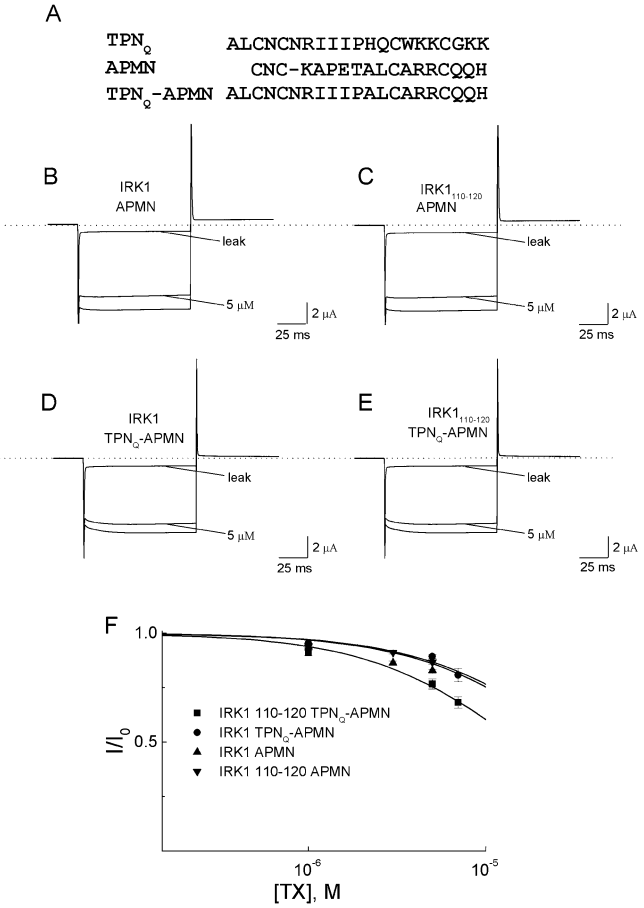

FIGURE 6: Inhibition of the wild-type and mutant IRK1 channels by honey bee toxins. (A) Sequences of TPN_Q, APMN, and their chimera. The N- and C-terminal halves of the chimeric toxin (TPN_Q-APMN) come from TPN_Q and APMN, respectively. (B−E) Currents of the wild-type and mutant IRK1 channels (the latter contain P110−P120 of ROMK1), recorded in the absence or presence of APMN or TPN_Q-APMN at the indicated concentrations. (F) Fraction of current not blocked (mean ± SEM; $n = 4$) plotted against the relevant toxin (TX) concentration. The curves through the data are fits of the equation described in Figure 2, yielding K_d values of 20.0 ± 0.1 and 20.0 ± 0.1 μM for the inhibition of wild-type and mutant IRK1 by APMN, and 20.0 ± 0.2 and 18.0 ± 0.3 μM for the inhibition of wild-type and mutant IRK1 by TPN_Q-APMN.

Identification of the Subunit in the GIRK1/4 Channel that Underlies High-Affinity Inhibition by TPN_Q. Cardiac Kir channels, gated by G proteins, consist of two different types of subunits, GIRK1 (Kir3.1) and GIRK4 (Kir3.4) (*33*, *34*, *39*). These heterotetrameric GIRK1/4 channels also exhibit high affinity for TPN_Q [apparent $K_d \sim 10$ nM; (*4*, *6*)]. If, as argued above, a competent variable region indeed suffices to confer high TPN_Q affinity upon the IRK1 channel, one expects to see a dramatic increase in the affinity of IRK1 for TPN_Q upon replacement of its variable region with that from either GIRK1, GIRK4, or both. To test this, we made two such mutant IRK1 channels called $IRK1_{GIRK1}$ and $IRK1_{GIRK4}$ (Figures 1 and 8A). Parts B−D of Figure 8 show currents of wild-type and mutant IRK1 channels in the absence or presence of TPN_Q at the concentrations indicated. Like wild-type IRK1, $IRK1_{GIRK1}$ is relatively insensitive to TPN_Q ($K_d = 20$ μM; Figure 8E). In contrast, $IRK1_{GIRK4}$ is rather sensitive ($K_d = 68$ nM). Furthermore, for reasons discussed below, we found that IRK1 acquires TPN_Q sensitivity when the C-terminal part of its variable region is from TPN_Q-sensitive GIRK4, even if the N-terminal part of the region is from TPN_Q-insensitive GIRK1 (Figure 9). These results confirm that a competent variable region confers toxin sensitivity upon a relatively insensitive channel and also suggest that GIRK4 but not GIRK1 underlies the high TPN_Q affinity of the heterotetrameric GIRK1/4 channel. The latter surmise is further supported by the finding described next.

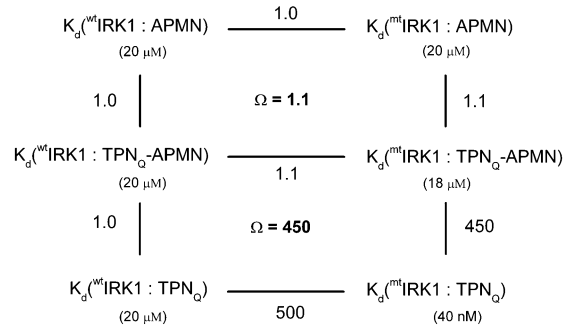

FIGURE 7: Thermodynamic mutant cycles. K_d values are for interactions between wild-type IRK1 and APMN (upper left), mutant IRK1 (containing P110−P120 of ROMK1) and APMN (upper right), wild-type IRK1 and TPN_Q-APMN chimera (middle left), mutant IRK1 and TPN_Q-APMN (middle right), wild-type IRK1 and TPN_Q (lower left), and mutant IRK1 and TPN_Q (lower right). For the top and bottom boxes, the Ω values are computed respectively as $K_d(^{wt}IRK1{:}TPN_Q\text{-}APMN)K_d(^{mt}IRK1{:}APMN)/K_d(^{mt}IRK1{:}TPN_Q\text{-}APMN)K_d(^{wt}IRK1{:}APMN) = 1.1$ and $K_d(^{wt}IRK1{:}TPN_Q)K_d(^{mt}IRK1{:}TPN_Q\text{-}APMN)/K_d(^{mt}IRK1{:}TPN_Q)K_d(^{wt}IRK1{:}TPN_Q\text{-}APMN) = 450$.

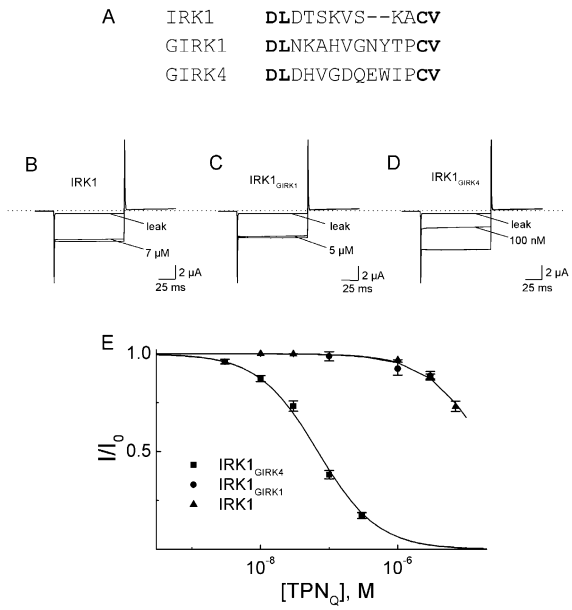

FIGURE 8: TPN_Q inhibition of IRK1 and its mutants containing the variable region from either GIRK1 or GIRK4. (A) Alignment of the variable region among IRK1, GIRK1, and GIRK4. (B−D) Currents of the wild-type and mutant IRK1 channels, recorded in the absence or presence of TPN_Q. In the mutant IRK1 channels ($IRK1_{GIRK1}$ or $IRK1_{GIRK4}$), the variable region is replaced by its counterpart from GIRK1 or GIRK4. (E) Fraction of current not blocked (mean ± SEM; $n = 4-5$) plotted against the TPN_Q concentration. The curves through the data are fits of the equation described in Figure 2, yielding K_d values of 20.0 ± 0.1 μM, 20.0 ± 0.2 μM, and 68.4 ± 0.4 nM for IRK1, $IRK1_{GIRK1}$, and $IRK1_{GIRK4}$, respectively.

Neither GIRK1 nor GIRK4 expresses effectively as a homotetrameric channel (*34*), yet together they form a functional channel with a 2:2 stoichiometry (*40*, *41*).

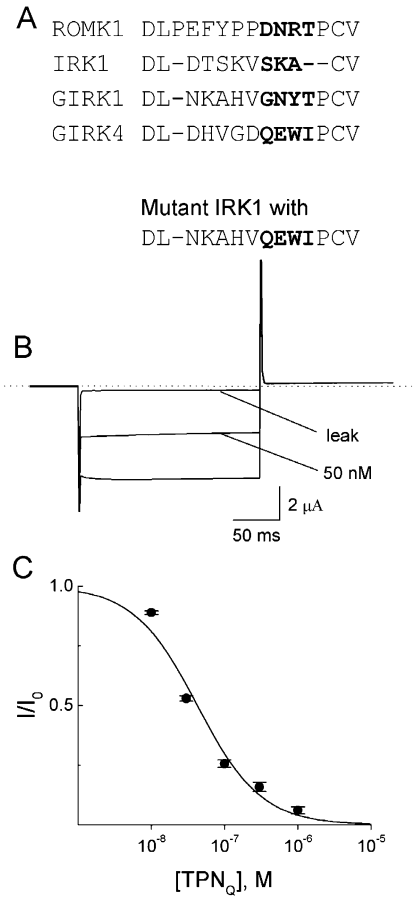

FIGURE 9: TPN_Q inhibition of IRK1 constructs whose proximal and distal parts of the variable region are replaced by those from GIRK1 and GIRK4. (A) Alignment of the variable region between ROMK1, IRK1, GIRK1, and GIRK4. (B) Currents of the mutant IRK1 channels, recorded in the absence or presence of TPN_Q. In the mutant, the proximal and distal parts of the variable region are replaced by their counterparts from GIRK1 (normal font) and GIRK4 (bolded), respectively. (C) Fraction of current not blocked (mean ± SEM; $n = 5$) plotted against the TPN_Q concentration. The curves through the data are fits of the equation described in Figure 2, yielding $K_d = 42.5 \pm 0.8$ nM.

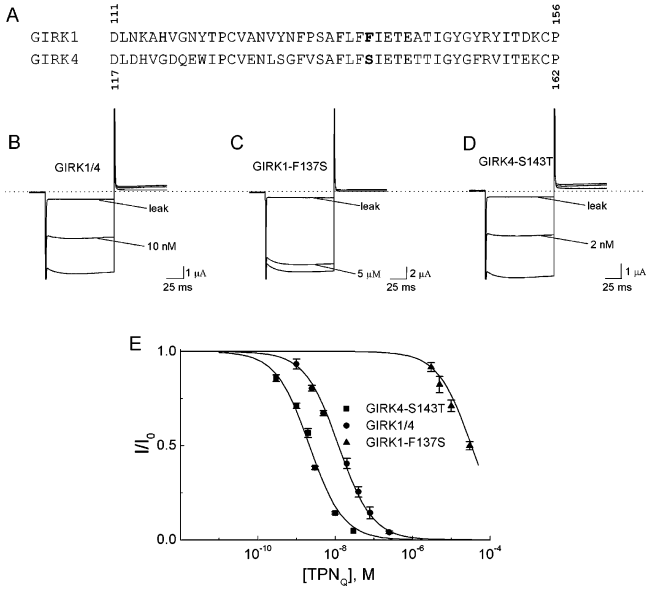

FIGURE 10: TPN_Q inhibition of GIRK1/4 heterotetramers and mutant GIRK1 or GIRK4 homomers. (A) Partial M1−M2 sequences of GIRK1 and GIRK4, where F137 of GIRK1 and S143 of GIRK4 are bolded. (B−D) Currents of GIRK1/4, GIRK1−F137S, and GIRK4−S143T, recorded in the absence or presence of TPN_Q at the concentrations indicated. (E) Fraction of current not blocked (mean ± SEM; $n = 5$) plotted against the TPN_Q concentration. The curves through the data are fits of the equation described in Figure 2, yielding K_d values of 12.2 ± 0.1 nM, 20.0 ± 0.2 μM, and 2.1 ± 0.2 nM for GIRK1/4, GIRK1−F137S, and GIRK4−S143T, respectively.

Interestingly, a single mutation located distally to the variable region (F137S in GIRK1 or S143T in GIRK4; Figure 10A) causes them not only to express functional homotetrameric channels, but also to conduct K^+ current constitutively (*42*). These two homotetrameric channels allow the TPN_Q sensitivity of GIRK1 and GIRK4 to be tested individually. Parts B−D of Figure 10 show current records of GIRK1/4, GIRK1−F137S, and GIRK4−S143T channels in the absence or presence of TPN_Q at the concentrations indicated. Consistent with the above findings, homomeric mutant GIRK1 is relatively insensitive to TPN_Q, whereas homomeric mutant GIRK4 is very sensitive. Analysis of dose-inhibition curves yields K_d values of 12 nM, 20 μM, and 2 nM for GIRK1/4, GIRK1−F137S, and GIRK4−S143T channels, respectively (Figure 10E). These results confirm that GIRK4 interacts with TPN_Q much more strongly than GIRK1.

DISCUSSION

Inward-rectifier K^+ channels play important roles in numerous vital physiological and pathophysiological processes and represent significant potential pharmacological targets. For example, cardiac GIRK1/4 channels mediate the vagal inhibition of pacemaker activity. Vagal release of acetylcholine (ACh) activates, via muscarinic receptors, G proteins, which in turn activate GIRK1/4 channels (*33*, *34*, *39*, *43*−*49*). The resulting K^+ conductance increase causes membrane hyperpolarization in the pacemaker cells and a slower heart rate. The muscarinic antagonist, atropine, administered to relieve the vagal inhibition of pacemaker activity (*50*), unfortunately produces profound general antimuscarinic side effects, which severely limit its clinical application. A selective inhibitor of the GIRK1/4 channel would therefore be highly desirable.

The action potential of cardiac myocytes has a characteristic plateau phase, which allows sufficient Ca^{2+} entry to trigger a forceful contraction. Forty years ago, Noble studied the role of strongly inwardly rectifying K^+ currents in the generation of cardiac action potentials and concluded that inward rectification causes a decrease in potassium conductance upon membrane depolarization, producing the long action-potential plateau, followed by an increase during repolarization, which accelerates the latter (*51*, *52*). Molecular genetic studies have identified the underlying channels as IRK1 (Kir2.1), and deletion of the IRK1 gene in mice results in prolonged action potentials (*53*). In light of these findings, a selective inhibitor for the IRK1 channel might provide a novel means to enhance cardiac contractility. Additionally, prolonging the action potential in both atrium and ventricle by inhibiting GIRK1/4 and IRK1 may extend the refractory period and therefore be potentially antiarrhythmogenic (*50*).

Despite these and other appealing reasons for developing specific inhibitors against medically significant Kir channels, serious doubts remain whether the various highly homologous Kir channels can in fact be selectively targeted. Specific

targeting requires two obvious conditions: the targeted channel sequence (or other structural feature) must differ sufficiently among the various channels, and binding of a specific ligand to the target region must result in a desirable functional alteration. The example we studied here satisfies both criteria. TPN_Q, a nonoxidizable derivative of a small toxin originally isolated from honey bee venom, interacts, through its C-terminal α helix, with the M1−M2 linker of Kir channels and inhibits some (e.g., ROMK1) with high affinity, whereas others (e.g., IRK1) are barely affected (*4*, *6*). We found that a short region in the N-terminal part of the M1−M2 linker in Kir channels is critical for high-affinity binding of TPN_Q (Figure 3). The region of only ∼10 residues varies in both length and sequence among various eukaryotic Kir channels, although the two pairs of residues (DL and CV) that flank the variable region are highly conserved (Figure 1).

Replacing the short region in IRK1 (relatively insensitive to TPN_Q) by its counterpart from highly sensitive ROMK1 renders the former channel sensitive (Figure 3). The apparent selectivity could mean either that the region forms the primary receptor for TPN_Q and/or that it merely hinders TPN_Q binding. Regarding possible hindrance, the two lysine residues in the variable region of IRK1 are conspicuous, because their positive charge may impede the binding of TPN_Q whose channel-interacting α helix contains several basic residues. However, replacing either or both lysines with alanine did not dramatically enhance the affinity of IRK1 for TPN_Q (Figure 4), nor did deleting the entire variable region (Figure 5). In contrast, results of the mutant cycle analysis are entirely consistent with the variable region interacting energetically with the C-terminal α helix of TPN_Q (Figure 7). This model also accounts for the previous finding that replacing the residues in the variable region of ROMK1, one at a time, with alanine dramatically alters the affinity of the channels for TPN_Q (*5*).

The bacterial channel KirBac1.1 lacks the variable region found in eukaryotic Kir channels (Figure 1) and so do many other types of K^+ channels such as bacterial MthK and KcsA or prokaryotic and eukaryotic Kv channels (Figure 1; refs *9*, *54*−*56*). Most significantly the seemingly accidental acquisition, during evolution, of the variable region by eukaryotic Kir channels creates a specific potential target in each channel type, which could be exploited for therapeutic purposes. Some Kir channels are, furthermore, hetero-tetramers (*33*, *34*, *39*), which entail additional target diversification. For example, in the case of the GIRK1/4 channel, only GIRK4 and not GIRK1 binds TPN_Q with high affinity (Figures 8−10).

Both the length and the sequence of the variable region are different among IRK1, GIRK1, GIRK4, and ROMK1 channels. Replacing the variable region in (relatively) TPN_Q-insensitive IRK1 (K_d = 20 μM) by that from sensitive channels GIRK4 or ROMK1 and not from insensitive GIRK1 renders IRK1 highly sensitive (Figures 3 and 8). The question thus arises why do only GIRK4 and ROMK1 and not GIRK1 and IRK1 exhibit high-affinity TPN_Q binding, even though the differences between any two of the four variable sequences are equally striking.

A possible clue lies in the α-helix-forming tendency of the four-residue sequences bolded in Figure 9A. The conspicuous absence of two distal residues in the variable region of low-affinity IRK1 suggests that a complete α-helical turn (at least four residues) is required for high TPN_Q affinity. If this were the case, the TPN_Q affinity of a given channel should correlate with the α-helix-forming tendency of the bolded four-residue sequences in the three Kir channels without missing residues. A common method for evaluating the α-helix-forming tendency of a given residue is to determine its energetically stabilizing (−) or destabilizing (+) effect on an α helix. Interestingly, our calculation with the experimentally determined energy values for individual residue types (*57*) shows that the sum of the α-helix-stabilizing energy of residues QEWI and DNRT (−1.0 and −1.2 kcal/mol) in the TPN-sensitive GIRK4 and ROMK1 channels is indeed comparable but much larger than that of GNYT (−0.3 kcal/mol) in TPN-insensitive GIRK1. Thus, although the exact energetics of TPN_Q binding to a channel are determined by interactions between residue pairs at their interface, an α-helical propensity of the four C-terminal residues in the variable region of the channel may be a prerequisite to any interaction with TPN_Q. If this is true, IRK1 should become TPN_Q sensitive provided its *C-terminal* residues in the variable region are replaced by those from TPN_Q-sensitive GIRK4, regardless of whether the N-terminal ones are from GIRK4 or TPN_Q-insensitive GIRK1. This is in fact what we observed (parts D and E of Figure 8 and parts B and C of Figure 9).

In summary, we have identified a short (∼10 residues) region in the distal part of the M1−M2 linker of Kir channels that is essential for high-affinity inhibition by TPN_Q. This region appears to form a critical part of the TPN_Q receptor and is present only in eukaryotic Kir channels and not in bacterial KirBac1.1. Both the length and the sequence of the region vary significantly among eukaryotic Kir channels. Thus, the appearance, during evolution, of the variable region in eukaryotic Kir channels offers an opportunity for selective targeting of medically significant Kir channels and raises the question whether any physiological ligands targeting the variable region evolved in parallel to modulate the Kir channel function. Additionally, we show that one can confer TPN_Q sensitivity onto Kir channels currently lacking inhibitors by replacing their variable region with that from a TPN_Q-sensitive channel. TPN_Q-sensitive mutant Kir channels will be useful in heterologous expression systems because currents of channels with acquired toxin sensitivity can then be readily separated from interfering background currents. Finally, we show that in the heteromeric GIRK1/4 channels the GIRK4 and not GIRK1 subunit actually confers high affinity for TPN.

ACKNOWLEDGMENT

We thank P. De Weer for critical review of our manuscript, K. Ho and S. Hebert for ROMK1 cDNA, L. Y. Jan for GIRK1 and IRK1 cDNAs, J. Yang for IRK1 cDNA subcloned in the pGEM-HESS vector, D. E. Clapham for GIRK4 (CIR) cDNA, and E. G. Peralta for the human muscarinic receptor cDNA.

REFERENCES

1. Stanfield, P. R., Nakajima, S., and Nakajima, Y. (2002) Constitutively active and G-protein coupled inward rectifier K^+ channels: Kir2.0 and Kir3.0, *Rev. Physiol., Biochem. Pharmacol. 145*, 50−179.

2. Hille, B. (2001) *Ion Channels of Excitable Membranes*, 3rd ed., Sinauer Associates, Inc., Sunderland, MA.
3. Ashcroft, F. M. (2000) *Ion Channels and Disease: Channelopathies*, 1st ed., Academic Press, San Diego, CA.
4. Jin, W., and Lu, Z. (1998) A novel high-affinity inhibitor for inward-rectifier K^+ channels, *Biochemistry 37*, 13291−13299.
5. Jin, W., Klem, A. M., Lewis, J. H., and Lu, Z. (1999) Mechanisms of inward-rectifier K^+ channel inhibition by tertiapin-Q, *Biochemistry 38*, 14294−14301.
6. Jin, W., and Lu, Z. (1999) Synthesis of a stable form of tertiapin: A high-affinity inhibitor for inward-rectifier K^+ channels, *Biochemistry 38*, 14286−14293.
7. Ramu, Y., Klem, A. M., and Lu, Z. (2002) Titration of tertiapin-Q inhibition of ROMK1 channels by extracellular protons, *Biochemistry 40*, 3601−3605.
8. Marker, C. L., Stoffel, M., and Wickman, K. (2004) Spinal G-protein-gated K^+ channels formed by GIRK1 and GIRK2 subunits modulate thermal nociception and contribute to morphine analgesia, *J. Neurosci. 24*, 2806−2812.
9. Doyle, D. A., Morais, C. J., Pfuetzner, R. A., Kuo, A., Gulbis, J. M., Cohen, S. L., Chait, B. T., and MacKinnon, R. (1998) The structure of the potassium channel: Molecular basis of K^+ conduction and selectivity, *Science 280*, 69−77.
10. Miller, C., Moczydlowski, E., Latorre, R., and Phillips, M. (1985) Charybdotoxin, a protein inhibitor of single Ca^{2+}-activated K^+ channels from mammalian skeletal muscle, *Nature 313*, 316−318.
11. Gimenez-Gallego, G., Navia, M. A., Reuben, J. P., Katz, G. M., Kaczorowski, G. J., and Garcia, M. L. (1988) Purification, sequence, and model structure of charybdotoxin, a potent selective inhibitor of calcium-activated potassium channels, *Proc. Natl. Acad. Sci. U.S.A. 85*, 3329−3333.
12. Garcia, M. L., Garcia-Calvo, M., Hidalgo, P., Lee, A., and MacKinnon, R. (1994) Purification and characterization of three inhibitors of voltage-dependent K^+ channels from *Leiurus quinquestriatus* var. *hebraeus* venom, *Biochemistry 33*, 6834−6839.
13. MacKinnon, R., and Miller, C. (1988) Mechanism of charybdotoxin block of the high-conductance, Ca^{2+}-activated K^+ channel, *J. Gen. Physiol. 91*, 335−349.
14. Miller, C. (1988) Competition for block of a Ca^{2+}-activated K^+ channel by charybdotoxin and tetraethylammonium, *Neuron 1*, 1003−1006.
15. MacKinnon, R., and Miller, C. (1989) Mutant potassium channels with altered binding of charybdotoxin, a pore-blocking peptide inhibitor, *Science 245*, 1382−1385.
16. MacKinnon, R., Heginbotham, L., and Abramson, T. (1990) Mapping the receptor site for charybdotoxin, a pore-blocking potassium channel inhibitor, *Neuron 5*, 767−771.
17. Bontems, F., Gilquin, B., Roumestand, C., Menez, A., and Toma, F. (1992) Analysis of side-chain organization on a refined model of charybdotoxin structural and functional implications, *Biochemistry 31*, 7756−7784.
18. Park, C. S., and Miller, C. (1992) Interaction of charybdotoxin with permeant ions inside the pore of a K^+ channel, *Neuron 9*, 307−313.
19. Stampe, P., Kolmakova-Partensky, L., and Miller, C. (1992) Mapping hydrophobic residues of the interaction surface of charybdotoxin, *Biophys. J. 62*, 8−9.
20. Escobar, L., Root, M. J., and MacKinnon, R. (1993) Influence of protein surface charge on the bimolecular kinetics of a potassium channel peptide inhibitor, *Biochemistry 32*, 6982−6987.
21. Stampe, P., Kolmakova-Partensky, L., and Miller, C. (1994) Intimations of K^+ channel structure from a complete functional map of the molecular surface of charybdotoxin, *Biochemistry 33*, 443−450.
22. Goldstein, S. A., Pheasant, D. J., and Miller, C. (1994) The charybdotoxin receptor of a Shaker K^+ channel: Peptide and channel residues mediating molecular recognition, *Neuron 12*, 1377−1388.
23. Stocker, M., and Miller, C. (1994) Electrostatic distance geometry in a K^+ channel vestibule, *Proc. Natl. Acad. Sci. U.S.A. 91*, 9509−9513.
24. Gross, A., Abramson, T., and MacKinnon, R. (1994) Transfer of the scorpion toxin receptor to an insensitive potassium channel, *Neuron 13*, 961−966.
25. Hidalgo, P., and MacKinnon, R. (1995) Revealing the architecture of a K^+ channel pore through mutant cycles with a peptide inhibitor, *Science 268*, 307−310.
26. Aiyar, J., Withka, J. M., Rizzi, J. P., Singleton, D. H., Andrews, G. C., Lin, W., Boyd, J., Hanson, D. C., Simon, M., and Dethlefs, B. (1995) Topology of the pore-region of a K^+ channel revealed by the NMR-derived structures of scorpion toxins, *Neuron 15*, 1169−1181.
27. Ranganathan, R., Lewis, J. H., and MacKinnon, R. (1996) Spatial localization of the K^+ channel selectivity filter by mutant cycle-based structure analysis, *Neuron 16*, 131−139.
28. Naranjo, D., and Miller, C. (1996) A strongly interacting pair of residues on the contact surface of charybdotoxin and a Shaker K^+ channel, *Neuron 16*, 123−130.
29. Gross, A., and MacKinnon, R. (1996) Agitoxin footprinting the Shaker potassium channel pore, *Neuron 16*, 399−406.
30. MacKinnon, R., Cohen, S. L., Kuo, A., Lee, A., and Chait, B. T. (1998) Structural conservation in prokaryotic and eukaryotic potassium channels, *Science 280*, 106−109.
31. Xu, X., and Nelson, J. W. (1993) Solution structure of tertiapin determined using nuclear magnetic resonance and distance geometry, *Proteins 17*, 124−137.
32. Kubo, Y., Baldwin, T. J., Jan, Y. N., and Jan, L. Y. (1993) Primary structure and functional expression of a mouse inward rectifier potassium channel, *Nature 362*, 127−133.
33. Kubo, Y., Reuveny, E., Slesinger, P. A., Jan, Y. N., and Jan, L. Y. (1993) Primary structure and functional expression of a rat G-protein-coupled muscarinic potassium channel, *Nature 364*, 802−806.
34. Krapivinsky, G., Gordon, E. A., Wickman, K., Velimirovic, B., Krapivinsky, L., and Clapham, D. E. (1995) The G-protein-gated atrial K^+ channel IKACh is a heteromultimer of two inwardly rectifying K^+ channel proteins, *Nature 374*, 135−141.
35. Peralta, E. G., Winslow, J. W., Peterson, G. L., Smith, D. H., Ashkenazi, A., Ramachandran, J., Schimerlik, M. I., and Capon, D. J. (1987) Primary structure and biochemical properties of an M2 muscarinic receptor, *Science 236*, 600−605.
36. Liman, E. R., Tytgat, J., and Hess, P. (1992) Subunit stoichiometry of a mammilian K^+ channel determined by construction of multimeric cDNAs, *Neuron 9*, 861−871.
37. Ho, K., Nichols, C. G., Lederer, W. J., Lytton, J., Vassilev, P. M., Kanazirska, M. V., and Hebert, S. C. (1993) Cloning and expression of an inwardly rectifying ATP-regulated potassium channel, *Nature 362*, 31−38.
38. Pease, J. H., and Wemmer, D. E. (1988) Solution structure of apamin determined by nuclear magnetic resonance and distance geometry, *Biochemistry 27*, 8491−8498.
39. Dascal, N., Lim, N. F., Schreibmayer, W., Wang, W., Davidson, N., and Lester, H. A. (1993) Expression of an atrial G-protein-activated potassium channel in *Xenopus* oocytes, *Proc. Natl. Acad. Sci. U.S.A. 90*, 6596−6600.
40. Silverman, S. K., Lester, H. A., and Dougherty, D. A. (1996) Subunit stoichiometry of a heteromultimeric G protein-coupled inward-rectifier K^+ channel, *J. Biol. Chem. 271*, 30524−30528.
41. Corey, S., Krapivinsky, G., Krapivinsky, L., and Clapham, D. E. (1998) Number and stoichiometry of subunits in the native atrial G-protein-gated K^+ channel IKACh, *J. Biol. Chem. 273*, 5271−5278.
42. Vivaudou, M., Chan, K. W., Sui, J.-L., Jan, L. Y., Reuveny, E., and Logothetis, D. E. (1997) Probing the G-protein regulation of GIRK1 and GIRK4, the two subunits of the K_{ACh} channel, using functional homomeric mutants, *J. Biol. Chem. 272*, 31553−31560.
43. Loewi, O. (1921) Über humorale Übertragbarkeit der Herznervenwirkung, *Pflügers Arch. 189*, 239−242.
44. Trautwein, W. and Dudel, F. (1958) Zum Mechanismus der Membranwirkung des Acetylcholin an der Herzmuskelfaser, *Pflügers Arch. 266*, 324−334.
45. Pfaffinger, P. J., Martin, J. M., Hunter, D. D., Nathanson, N. M., and Hille, B. (1985) GTP-binding proteins couple cardiac muscarinic receptors to a K channel, *Nature 317*, 536−538.
46. Breitwieser, G. E., and Szabo, G. (1985) Uncoupling of cardiac muscarinic and β-adrenergic receptors from ion channels by a guanine nucleotide analogue, *Nature 317*, 538−540.
47. Logothetis, D. E., Kurachi, Y., Galper, J., Neer, E. J., and Clapham, D. E. (1987) The $\beta\gamma$ subunits of GTP-binding proteins activate the muscarinic K^+ channel in heart, *Nature 325*, 321−326.
48. Wickman, K. D., Iniguez-Lluhl, J. A., Davenport, P. A., Taussig, R., Krapivinsky, G. B., Linder, M. E., Gilman, A. G., and Clapham, D. E. (1994) Recombinant G-protein $\beta\gamma$-subunits

activate the muscarinic-gated atrial potassium channel, *Nature 368*, 255−257.
49. Reuveny, E., Slesinger, P. A., Inglese, J., Morales, J. M., Iniguez-Lluhi, J. A., Lefkowitz, R. J., Bourne, H. R., Jan, Y. N., and Jan, L. Y. (1994) Activation of the cloned muscarinic potassium channel by G protein $\beta\gamma$ subunits, *Nature 370*, 143−146.
50. *Goodman & Gilman's The Pharmacological Basis of Therapeutics* (1996) (Hardman, J. G., Limbird, L. E., Molinoff, P. B., Ruddon, R. W., and Gilman, A. G., Eds.) 9th ed., McGraw-Hill, New York.
51. Noble, D. (1962) A modification of Hodgkin−Huxley equations applicable to Purkinje fibre action and pace-maker potentials, *J. Physiol. 160*, 317−352.
52. Noble, D. (1965) Electrical properties of cardiac muscle attributable to inward going (anomalous) rectification, *J. Cell. Comp. Physiol. 66*, 127−136.
53. Zaritsky, J. J., Redell, J. B., Tempel, B. L., and Schwarz, T. L. (2001) The consequence of disrupting cardiac inwardly rectifying K^+ current (*I*K1) as revealed by the targeted deletion of the murine *Kir2.1* and *Kir2.2* genes, *J. Physiol. 533*, 697−710.
54. Schrempf, H., Schmidt, O., Kümmerlen, R., Hinnah, S., Müller, D., Betzler, M., Steinkamp, T., and Wagner, R. (1995) A prokaryotic potassium ion channel with two predicted transmembrane segments from *Streptomyces lividans*, *EMBO J. 14*, 5170−5178.
55. Jiang, Y., Lee, A., Chen, J., Cadene, M., Chait, B. T., and MacKinnon, R. (2002) Crystal structure and mechanism of a calcium-gated potassium channel, *Nature 417*, 515−522.
56. Ruta, V., Jiang, Y., Lee, A., Chen, J., and MacKinnon, R. (2003) Functional analysis of an archaebacterial voltage-dependent K^+ channel, *Nature 422*, 180−185.
57. Creighton, T. E. (1993) *Proteins: Structures and Molecular Properties*, 2nd ed., W. H. Freeman and Company, New York.

BI049125X